Bioorganic & Medicinal Chemistry 18 (2010) 1789–1797

Contents lists available at ScienceDirect

Bioorganic & Medicinal Chemistry

journal homepage: www.elsevier.com/locate/bmc

# Colony stimulating factor-1 receptor as a target for small molecule inhibitors

Baratali Mashkani [a], Renate Griffith [b,*], Leonie K. Ashman [a,c]

[a] School of Biomedical Sciences, University of Newcastle, Callaghan, NSW 2308, Australia
[b] School of Environmental and Life Sciences, University of Newcastle, Callaghan, NSW 2308, Australia
[c] Hunter Medical Research Institute, Newcastle, Australia

ARTICLE INFO

*Article history:*
Received 12 November 2009
Revised 21 January 2010
Accepted 22 January 2010
Available online 28 January 2010

*Keywords:*
Binding mode
Kinase inhibition
Flexible docking
Kinase domain conformation
Drug design

ABSTRACT

Imatinib, dasatinib, sunitinib, CEP-701, and PKC-412, ATP-competitive small molecule inhibitors of type III receptor tyrosine kinases c-KIT and/or FLT3, were evaluated for binding to the closely related receptor, FMS, by docking into models of inactive and active conformations of the FMS kinase domain. To confirm the docking predictions, the drugs were tested for their activity and selectivity in inhibiting cell proliferation and FMS phosphorylation upon stimulation by the FMS ligand, CSF-1. All five drugs inhibited FMS activity. Imatinib, dasatinib and CEP-701 represent three different types of interactions determining drug potency and selectivity.



## 1. Introduction

Macrophage colony stimulating factor (CSF-1) receptor (FMS), along with KIT, FLT3, PDGFRα and β, is a member of the receptor tyrosine kinase (RTK) type III family, characterised by five immunoglobulin-like extracellular domains and a kinase insert dividing the intracellular kinase domain into two lobes.[1] FMS and its ligand CSF-1 have been implicated in a wide range of physiological and pathological processes. For example, FMS is required for development, survival, proliferation, and differentiation of the monocyte-macrophage series[2] and for prostate development.[3] FMS and CSF-1 expression increase significantly in the epithelial cells of mammary glands in response to glucocorticoid hormones and they are required for normal development of mammary glands during pregnancy and lactation.[4] CSF-1 is believed to promote pro-atherogenic signalling and progression of plaques by stimulation of macrophages in the plaques.[5]

CSF-1 not only activates FMS expressing cells, especially macrophages, it is also a chemotactic factor causing recruitment and activation of macrophages to CSF-1 producing tissues including tumours, transplanted organs and tissues affected by autoimmune diseases. CSF-1 produced by synovial fibroblasts induces differentiation of synovial macrophages into osteoclasts causing bone destruction in rheumatoid arthritis patients.[6] Activation of tumour-associated macrophages (TAMs) results in both positive and negative outcomes for tumour growth. CSF-1 activated macrophages may have higher activity against tumours, but they may promote tumour growth through expression of higher levels of growth factors, stimulation of angiogenesis and promotion of metastasis by secretion of matrix degrading enzymes.[7] There is a correlation between CSF-1 expression level and invasiveness in human breast cancer cell lines[8] and tissue microarray analysis showed that expression of FMS is associated with poor prognosis of breast cancer.[9] While FMS it is not detectable in normal prostate or benign hypertrophy, it is expressed in human samples of intra-epithelial neoplasia or carcinoma with Gleason grade of 3 or 4,[3] and prostate carcinoma cell lines (DU-145, PC-3, and LNCaP) express both FMS and its ligand, CSF-1.[10]

Blockade of the FMS kinase may be a helpful treatment strategy in a variety of cancers and inflammatory diseases. Small molecule tyrosine kinase inhibitors (SMIs) imatinib and dasatinib have been reported to suppress differentiation of monocytes into tumour-associated macrophages and osteoclasts[11–14] and may have therapeutic application for prevention of breast and prostate cancer metastasis. Imatinib as a FMS inhibitor has been shown to suppress metastasis of breast cancer to bones by deactivation of osteoclasts.[15] Dasatinib was used for targeting Src family kinases (SFK) in prostate cancer treatment,[16] but as it can inhibit both FMS and Src, inhibition of FMS may contribute to treatment effects.

Inhibition of the kinase domain using SMIs is the most practical approach to target aberrant kinase activity. Most SMIs compete with ATP in binding to the ATP-binding pocket and stabilise the inactive kinase domain conformation. Imatinib, an inhibitor of the Bcr/Abl fusion protein, was the first successful SMI, developed originally for treatment of chronic myeloid leukaemia.[17] It has now

* Corresponding author at present address: School of Medical Sciences, Department of Pharmacology, University of New South Wales, UNSW Sydney, NSW 2052, Australia. Tel.: +61 2 9385 1912; fax: +61 2 9385 1059.
*E-mail address:* r.griffith@unsw.edu.au (R. Griffith).

0968-0896/$ - see front matter Crown Copyright © 2010 Published by Elsevier Ltd. All rights reserved.
doi:10.1016/j.bmc.2010.01.056

been found that imatinib inhibits other kinases including FMS and KIT.[18,19] Because of high similarity in the ATP-binding site, low selectivity is a common problem with existing kinase inhibitors. However, variations can be identified by structural analysis and could be utilised to design highly selective inhibitors. For example, Thr663 (FMS) and Thr670 (KIT) are necessary for imatinib binding and mutation of this Thr to Ile (Thr670Ile) in KIT results in imatinib resistance.[20]

Because of the high homology of type III RTKs, some known SMIs of KIT or FLT3 kinases were tested for their ability to interact with FMS in this study. In the absence of crystal structures for these molecules in complex with the FMS protein, modelling and docking were performed to predict possible interactions between the drugs and FMS. The results of the structural analysis were correlated with potency and selectivity data obtained for the drugs in a cell-based assay. The structure–activity relationships determined here will be useful in designing more potent and selective drugs for treatment of chronic diseases associated with FMS where minimisation of side effects due to inhibition of a broad range of kinases is of crucial importance.

## 2. Results

### 2.1. Docking of small molecule kinase inhibitors into FMS structure

#### 2.1.1. Validation of the docking procedure

The docking procedure was validated by docking the ligands imatinib, the arylamide molecule, sunitinib, and dasatinib (see Fig. 1 for structures) back into their corresponding crystal structures (see Table 1 for docking results).

All docked poses of imatinib (100%) were in one cluster with average docked energy of −15.94 kcal/mol. Structural analysis of the docked poses shows hydrogen bond formation between imatinib and Cys673, Thr670 and Asp810 in KIT, which is very similar to the hydrogen bonding in the crystal structure, 1T46.[21]

Docking of the arylamide molecule back into the FMS kinase also yielded very similar results to the crystal structure, 2I1M.[22] The majority of poses (90%) are in the first cluster with average docking energy of −11.71 kcal/mol. A hydrogen bond with the nitrogen of the backbone of Cys666 is a common feature among all poses in this cluster. Other hydrogen bonds may be formed with the side chains of Cys666 or Tyr665, resembling the interactions in the 2I1M crystal structure. In addition, structural analysis showed a π–π interaction between the side chain of Tyr665 and the central aromatic ring of the arylamide molecule.

The chlorine (Cl) atom in dasatinib was replaced by a methyl group ($CH_3$), and the new molecule named 'dacatinib' (see Fig. 1) was used for docking to keep the number of atom types within the limitations of AutoDock 3.05. Most of the docking poses of dacatinib in Abl kinase (70%) were in the correct orientation with average docking energies of −13.80 to −13.07 kcal/mol (Table 1). Structural analysis showed that modification of the dasatinib molecule did not affect the docking outcome. Dacatinib was docked into Abl kinase similar to the Abl/dasatinib crystal structure, 2GQG,[23] and formed three hydrogen bonds with the residues Met318 (2×) and Thr315. Additionally, π–π and π-cation interactions are present between dacatinib and the sidechains of

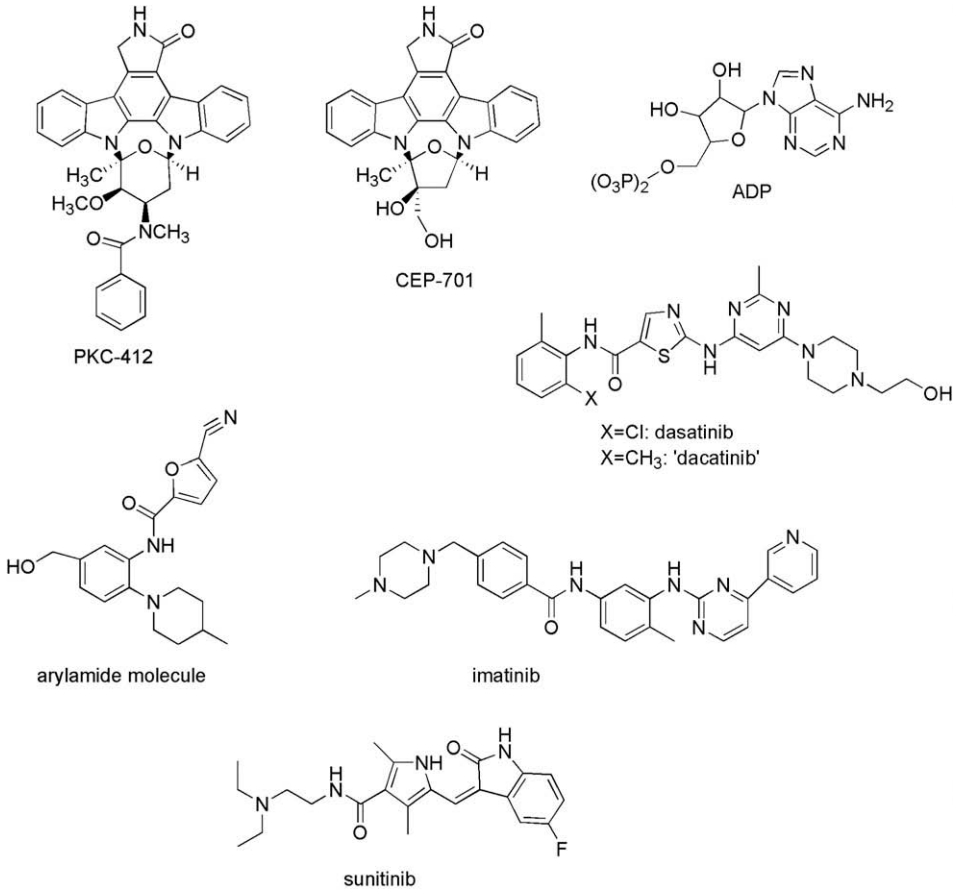


**Figure 1.** Structures of small molecule inhibitors used in this study as well as ADP and the arylamide molecule. * The Cl in dasatinib was replaced with $CH_3$ ('dacatinib') for docking analysis with AutoDock.

**Table 1**
Summary of docking results

| Receptor name (conformation) | Ligand | % of poses in largest cluster | Mean docked energy of largest cluster (kcal/mol) | Protein residues involved in hydrogen bonds |
|---|---|---|---|---|
| KIT (1T46[21]) (inactive) | Imatinib | 100 | −15.9 | Cys673, Thr670, Asp810 |
| FMS model based on 1T46 (inactive) | Imatinib | 58 | −15.6 | Cys666, Asp796 and π-cation interaction with His776 |
| FMS M637L Model based on 1T46 (inactive) | Imatinib | 97 | −15.8 | Cys666, Thr663, Glu633 and π-cation interaction with Lys616 |
| FMS (2I1M2[22]) (inactive) | Arylamide | 90 | −11.7 | Cys666, Tyr665 |
| FMS (2I1M2) (inactive) | CEP-701 | 100 | −12.6 | Cys666 (2×), Ala800 |
| FMS model based on 1PKG[25] (active) | CEP-701 | 100 | −13.5 | Cys666, Arg801 (2×) and π–π interaction withTyr665 |
| FMS model based on 1PKG (active) | PKC-412 | 86 | −7.7 | Cys666, Glu664, Ala800 and π–π interaction with Tyr665 |
| KIT (3G0E[24]) (inactive) | Sunitinib | 33, 8 | −11.3, −11.4 | Cys673 |
| FMS model based on (3G0E) (inactive) | Sunitinib | 19 | −11.3 | No hydrogen bonds |
| Abl (2GQG[23]) (active) | Dacatinib | 24, 18, 16, 12 | −13.8 to −13.1 | Met318 (2×), Thr315, π–π and π-cation interactions withPhe317 and Lys271, poses differ in 'tail' arrangement |
| FMS model based on 2GQG (active) | Dacatinib | 43, 25 | −13.3 and −13.0 | Cys666, Thr663 and π–π and π-cation interactions withTyr665 and Lys616 |

Phe317 and Lys271, respectively. Flexibility of the dacatinib molecule in docking allows the 'tail' of dacatinib (the piperazine ring with its ethanol substituent) to adopt different orientations.

Sunitinib was docked back into the crystal structure of the sunitinib/KIT complex (3G0E[24]) with only moderate success. Only two poses in clusters with a total of 41% of all poses and mean docking energies of −11.33 and −11.40 kcal/mol (Table 1) were similar to the orientation of sunitinib in the crystal structure. Sunitinib is not fully resolved in the 3G0E crystal structure, the flexible tail around the tertiary amine group is not visible.

### 2.1.2. FMS structures used for docking

The crystal structure of FMS with an arylamide molecule 2I1M[22] was used for docking of CEP-701 and PKC-412 because of its high resolution and structural similarity between the arylamide molecule, CEP-701 and PKC-412 (Fig. 1). Small modifications were made to the 2I1 M crystal structure by removing the arylamide molecule and residues 547–556 which are part of the FMS juxtamembrane domain, which interfere with docking of the SMIs in the region surrounded by the α-C helix and the activation loop. Homology models of FMS built based on KIT (1T46 and 3G0E[24]) and Abl kinases (2GQG) were used for docking of imatinib, sunitinib and dacatinib respectively.

### 2.1.3. Docking of CEP-701 and PKC-412 into FMS

Docking of CEP-701 into the crystal structure of FMS (2I1M) showed that CEP-701 fitted into the hinge region of FMS with 100% of poses in one cluster and average docking energy of −12.61 kcal/mol (Table 1). CEP-701 formed three hydrogen bonds, two with Cys666 in the hinge region and one with Ala800 at the start of the activation loop, as well as a hydrophobic interaction with Leu785 (Fig. 2, panel A). Superimposition showed that docked CEP-701 (in green, Fig. 2, panel B) and the arylamide molecule in 2I1M (in red) can be overlaid very well and that the functional groups are in the same orientations.

PKC-412 cannot be docked into the cleft between the two kinase lobes in 2I1M. PKC-412 contains larger groups on the side of the molecule opposite to the lactam ring (see Fig. 1) compared to CEP-701. These groups cannot be accommodated and clash with residues of the activation loop near Ala800 (data not shown).

The FMS structure 2I1M resembles an inactive kinase domain conformation. We also successfully docked CEP-701 and PKC-412 into the active conformation of FMS generated by homology modelling based on KIT, 1PKG[25] (Table 1). The only cluster of CEP-701 docked into the active conformation of FMS contains 100% of poses with mean docking energy of −13.45 kcal/mol which shows some improvement compared to docking into the inactive conformation. CEP-701 forms one hydrogen bond with Cys666, and two hydrogen bonds with Arg801, as well as a π–π interactions with Tyr665 (Table 1). Docking of PKC-412 into the active conformation of FMS was possible and led to a very similar pose to the one for CEP-701. PKC-412 formed three hydrogen bonds and the same π–π interaction as CEP-701 (Table 1). The docking energy, however, was much reduced due to steric clashes. An example illustrating docking of PCK-412 (in red) superimposed onto ADP in the active KIT conformation (in green) is shown in Figure 2, panel C.

### 2.1.4. Docking of imatinib into FMS

Imatinib could not be docked into the FMS crystal structure (2I1M) and therefore an FMS model based on the KIT crystal structure with imatinib (1T46) was examined. Docked poses of imatinib in this structure formed four clusters. The largest cluster with 58% of poses had slightly less favourable docking energy (−15.64 kcal/mol) (Table 1) compared to the first cluster with 39 members and average energy of −15.95 kcal/mol. Structural analysis (Fig. 2, panel D) showed that the lowest energy pose in the first cluster (in green) was in an inverted orientation and could not form any of the expected hydrogen bonds with FMS residues (compared to imatinib in the KIT crystal structure). However, the second cluster (in red) is in a similar orientation to imatinib in the KIT crystal structure and forms hydrogen bonds with Cys666 and Asp796 of the DFG motif, but not with Thr663. A π-cation interaction with His776 is also observed.

Sequence identity or similarity between the kinase domains of KIT and FMS is 69% and 78%, respectively, and when 1T46 and the FMS model based on 1T46 were superimposed, the overall structures were very similar with root mean square deviation (RMSD) of 0.58. Thus, it was expected that docking of imatinib into the FMS model based on 1T46 would result in a very similar pose to the crystal structure. However, analysis of residues close to imatinib in the superimposed structures of KIT and FMS showed that two residues are different in the imatinib binding pocket. Leu644 and Cys809 (KIT) have been replaced by Met637 and Gly795 in FMS. The side chain of Gly795 is smaller than Cys809, which means that Gly795 should not interfere with binding of imatinib. On the other hand, Met637 in FMS has a larger side chain

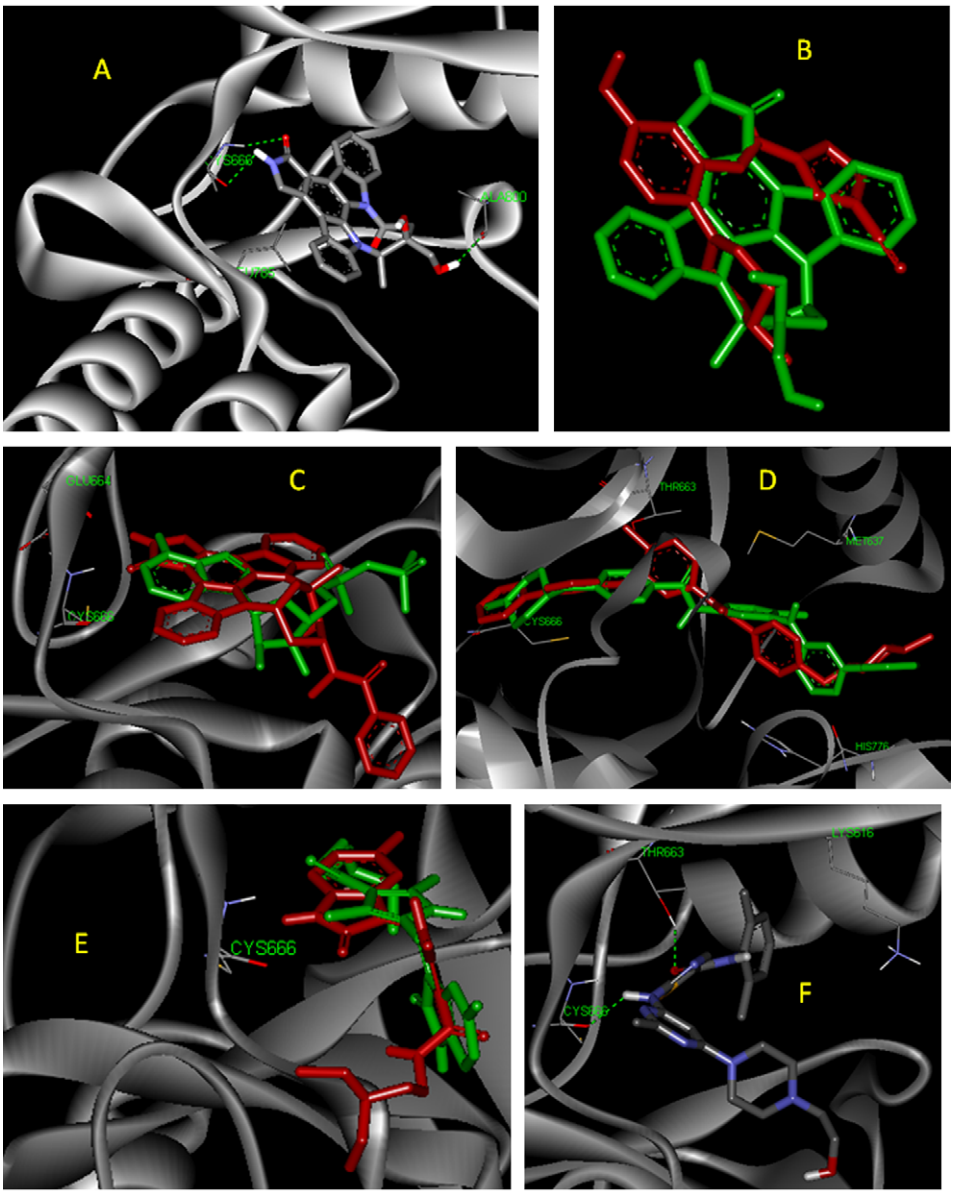


**Figure 2.** Docking results for small molecule inhibitors into the FMS kinase domain. Display of residues Lys586-Glu598 in the nucleotide binding loop has been turned off in panels **A**, **C**, and **F** to show the position of the inhibitors in the hinge region. Protein backbones are displayed as ribbons with selected side chains shown as lines, colour-coded by element: N in blue, O in red, H in white, C in grey, and S in yellow. The inhibitors are illustrated as sticks. In panels **A** and **F** the sticks are colour-coded by element: N in blue, O in red, H in white, C in grey, and S in yellow. Hydrogen bonds are shown by green, dashed lines. Panel **A**: CEP-701 docked into the FMS crystal structure (2I1M[22]). Panel **B**: CEP-701 (green) docked into 2I1 M superimposed on the arylamide molecule (red) in complex with FMS in 2I1 M. Panel **C**: PKC-412 (in red) docked into the active conformation of FMS (homology model based on KIT, 1PKG[25]) superimposed on ADP (green) as found in KIT in 1PKG. Panel **D**: Imatinib docked into the FMS model based on KIT, 1T46.[21] The energetically most favourable poses in clusters 1 and 2 are in green and red, respectively. Panel **E**: Sunitinib docked into the FMS model based on KIT, 3G0E.[24] The pose resembling sunitinib in 3G0E is coloured red, the inverted orientation found in the majority of poses is coloured green. Panel **F**: Dacatinib docked into the FMS model based on Abl, 2GQG.[23]

than Leu644 in KIT and may be preventing imatinib from being docked into FMS in the same orientation as it was docked into KIT. To test this, imatinib was docked into a homology model based on 1T46 of the M837L FMS mutant. Almost all of the poses (97%) were in one cluster with mean docking energy of −15.77 kcal/mol. Structural analysis of the lowest energy poses in that cluster showed three hydrogen bonds between imatinib and FMS residues Cys666, Thr663 and Glu633, as well as one π-cation interaction between Lys616 and the aromatic ring (with a methyl substitution) in the middle of imatinib (not shown). Thus, imatinib can be docked into this mutant in a very similar fashion to its interactions with KIT in the 1T46 crystal structure. Imatinib cannot be docked into the model of the active FMS kinase domain conformation built based on 1PKG (data not shown).

### 2.1.5. Docking of sunitinib into FMS

Because we found with imatinib that it was preferable to dock into a model based on a crystal structure containing the same compound, sunitinib was docked into an FMS model based on the crystal structure of KIT in complex with this drug (3G0E[24]). The cluster resembling the position of sunitinib in 3G0E contained 19% of docked sunitinib poses into FMS with docking energy of −11.26 kcal/mol (Table 1; red structure in Fig. 2, panel E). Sunitinib made, however, no hydrogen bonds in this pose, only a π–π interaction with Tyr665. The majority of poses (62%) showed sunitinib docked into FMS in an inverted manner, with the flexible amine tail interacting with the hinge region (green in Fig. 2, panel E). In light of these results, and the relatively poor docking of sunitinib into 3G0E, we also attempted to dock sunitinib into the FMS crystal

structure in complex with the arylamide molecule, 2I1M. As expected, sunitinib does not fit into the pocket in 2I1M (data not shown). Sunitinib also cannot be docked into the ADP binding pocket in the model of the active FMS kinase domain conformation built based on 1PKG (data not shown).

#### 2.1.6. Docking of dacatinib into FMS

Dacatinib was docked into an FMS model based on a crystal structure of the Abl kinase with dasatinib (2GQG) in which the kinase domain is in the active conformation. Results were very similar to the original structure of 2GQG. The largest cluster of docked poses (43%) also had the most favourable average docking energy of −13.27 kcal/mol. Dacatinib forms hydrogen bonds with Thr663 and Cys666 in the hinge region, as well as a π-cation interaction with Lys616 (Fig. 2, panel F). Another cluster of 25 poses with average docking energy of −13.04 kcal/mol resembles the crystal structure even more closely and forms the same hydrogen bonds, as well as the π-cation interaction and an additional π–π interaction with Tyr665. The two poses also differ in the arrangement of the flexible tail. We also docked dacatinib into a model of the active conformation FMS based on KIT 1PKG; it docked differently, and poorly (data not shown).

### 2.2. Inhibition of FD-FMS cell proliferation by kinase inhibitors

To test the validity of the docking results, a cell-based assay system similar to one previously used to study c-KIT mutants,[26] was developed by expressing human FMS in growth factor-dependent murine FDC-P1 cells (FD-FMS assay system). The FD-FMS cells grow in the presence of either human CSF-1 or mouse granulocyte macrophage colony stimulating factor (GM-CSF). Comparison of the effects of inhibitors on proliferation of cells in CSF-1 and GM-CSF provides initial information on the selectivity of the drug for inhibition of FMS kinase activity. Treatment of FD-FMS cells with CEP-701, dasatinib, imatinib, PKC-412, sunitinib, and the Src family kinase inhibitor SU6656 all resulted in inhibition of cell proliferation in response to CSF-1 (Fig. 3). Dasatinib, imatinib and sunitinib selectively inhibited proliferation in CSF-1 compared to GM-CSF, whereas CEP-701, PKC-412 and SU6656 also potently inhibited the response to GM-CSF. Comparison of the concentration of drug required to halve the FD-FMS cell proliferation ($IC_{50}$) with CSF-1 or GM-CSF gives an indication of how effective the drug is against FMS compared to the unrelated GM-CSF receptor and/or downstream signalling pathways (Table 2).

Dasatinib was the most potent inhibitor of CSF-1 dependent proliferation and appeared to be highly selective for FMS as proliferation in GM-CSF was unaffected at concentrations up to 500 nM. Similarly, sunitinib and imatinib showed strong selectivity for inhibition of FMS signalling in this assay. Receptor tyrosine kinases including FMS are known to activate Src family kinases and dasatinib is a known inhibitor of Src family kinases (SFKs).[27] Therefore, SU6656, a well-characterised SFK inhibitor[28] provided an important control for this experiment to compare potency of dasatinib against FMS and SFKs. SU6656 inhibited cell growth in the presence of CSF-1 and GM-CSF, suggesting that both FMS and GM-CSF receptors are dependent on signalling through SFKs to promote cell proliferation. However, at the concentrations used in these experiments, dasatinib did not inhibit growth in GM-CSF indicating that its effect on FMS signalling cannot be attributed to inhibition of an associated SFK.

CEP-701 did not selectively inhibit FMS-dependent proliferation while PKC-412 showed only slight selectivity. GM-CSF receptor, unlike FMS, does not have intrinsic kinase activity and a JAK2 tyrosine kinase molecule constitutively associated with its β subunit is responsible for initiation of the signalling response after binding of GM-CSF with the α subunit of the receptor.[29] Although their structures are different, FMS and GM-CSF receptor share several downstream signalling pathways. The data indicate that PKC-412 and CEP-701 inhibit FMS, JAK2 and/or common downstream pathways required for cell proliferation and/or survival.

### 2.3. Inhibition of FMS phosphorylation by small molecule inhibitors

A more direct way to test for inhibition of RTK signalling is to determine the effect of a drug on autophosphorylation which accompanies receptor activation.[1] This was done by probing western blots of electrophoretically separated lysates of CSF-1-stimulated FD-FMS cells with antibodies to phosphotyrosine (as previously described for KIT).[26,30] Treatment of FD-FMS cells with

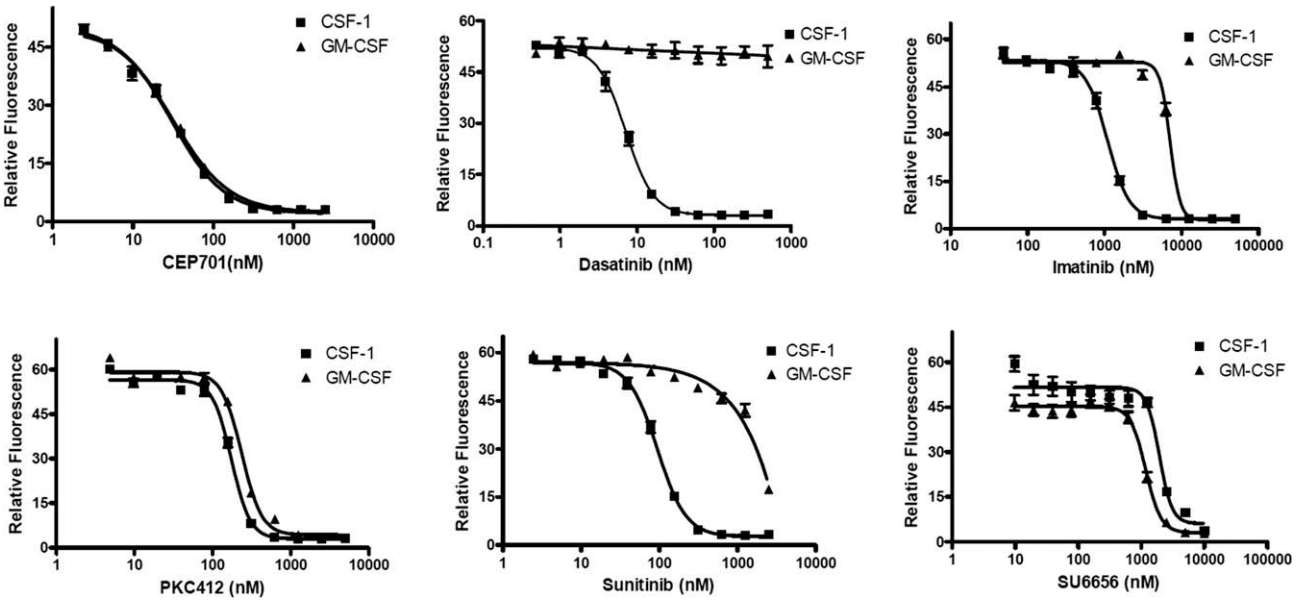


**Figure 3.** Effect of small molecule inhibitors on proliferation of FD-FMS cells. Cells were cultured in the presence of the indicated concentrations of drugs with either GM-CSF or CSF-1 as growth factor. After 48 h the relative number of viable cells per well was determined based on fluorescence of resofurin produced by reduction of resazurin. Data points are shown as mean ± SD of four replicate wells. The figure shows a representative of three independent experiments.

**Table 2**
FMS inhibitory activities

| | $Log_{10}IC_{50}$ in GM-CSF[a] | $Log_{10}IC_{50}$ in CSF-1[a] | $IC_{50}$ in GM-CSF (nM) | $IC_{50}$ in CSF-1 (nM) | $IC_{50}$ in GM-CSF/$IC_{50}$ in CSF-1 | *P* value[b] |
|---|---|---|---|---|---|---|
| CEP-701 | 1.43 ± 0.05 | 1.49 ± 0.07 | 26 | 31 | 0.8 | 0.256 |
| Dasatinib | >2.70 | 0.87 ± 0.03 | >500 | 7.4 | >67 | 0.000 |
| Imatinib | 3.92 ± 0.11 | 3.10 ± 0.09 | 8437 | 1274 | 6.6 | 0.006 |
| PKC-412 | 2.29 ± 0.13 | 2.15 ± 0.10 | 200 | 142 | 1.4 | 0.213 |
| Sunitinib | >3.08 | 2.18 ± 0.12 | >1000 | 155 | >7.7 | 0.000 |

[a] $Log_{10}IC_{50}$ ± SD as calculated from the experiment shown in Figure 3 plus two additional independent experiments using GraphPad Prism 4.3 software. $IC_{50}$ in nM.
[b] The $IC_{50}$ values of three individual experiments in GM-CSF and CSF-1 were compared using *t*-test and the results are shown as *p*-values.

different concentrations of CEP-701, sunitinib, dasatinib, imatinib, or PKC-412 before stimulation by CSF-1 caused dose-dependent disruption of FMS autophosphorylation as described before for KIT[30] (Fig. 4). The data showed that CEP-701 and PKC-412 substantially decreased FMS tyrosine phosphorylation at concentrations comparable to their $IC_{50}$ values in the cell proliferation assay. This demonstrates that these compounds do indeed inhibit FMS kinase activity and suggests that direct FMS inhibition by CEP-701 and PKC-412 may contribute to cell growth inhibition in CSF-1 even though other targets are also involved.

Concentrations of imatinib, sunitinib and dasatinib required to decrease the tyrosine phosphorylation down to around 50% of that in CSF-1 stimulated controls were similar to their $IC_{50}$ values in cell proliferation assays consistent with their selectivity for FMS. SU6656 was also tested for its effect on FMS autophosphorylation in cells stimulated with CSF-1 to investigate the role of SFK inhibition in the action of dasatinib. SU6656 did not cause reduction in tyrosine phosphorylation of FMS even at concentrations above its $IC_{50}$ in the cell proliferation assay (Fig. 5). Therefore, the reduction in FMS tyrosine phosphorylation by dasatinib is not primarily due to inhibition of an associated SFK, confirming the direct action of this compound on FMS kinase.

## 3. Discussion

Application of small molecules competing with ATP is a common treatment strategy for diseases associated with aberrant activity of protein tyrosine kinases. The idea of using ATP-competitive inhibitors was challenged initially because high similarity between ATP-binding pockets was predicted to result in severe side effects due to inhibition of multiple kinases. However, the development of imatinib demonstrated the possibility of selectively inhibiting kinases. Although further investigation showed that imatinib inhibits a number of kinases, including FMS, KIT and PDGFR,[18,19] its known range of activity remains limited.

To understand the mode of binding of several known kinase inhibitors to the FMS kinase domain, we combined computer-aided docking methods with experimental determination of inhibition of kinase activity. Our docking software, AutoDock3, like most docking programs, cannot consider protein flexibility. Introducing side chain flexibility into the latest version of the software, AutoDock4, requires much more computational power. Our initial attempts to use AutoDock4 were unsuccessful. By increasing the population size and number of energy evaluations in AutoDock3, we could successfully reproduce the crystallographic conformations and orientations of the ligands in four different kinase domain/inhibitor complexes. In each case, the correct binding mode was in the largest cluster of poses, accounting for at least 41% of all poses found.

A major challenge for docking arises from the large conformational changes undergone by kinases on activation and their resultant effects on inhibitor binding.[31] To compensate for the inability to treat the protein as flexible, we used a novel, 'flexible docking' approach by docking each inhibitor into a number of different

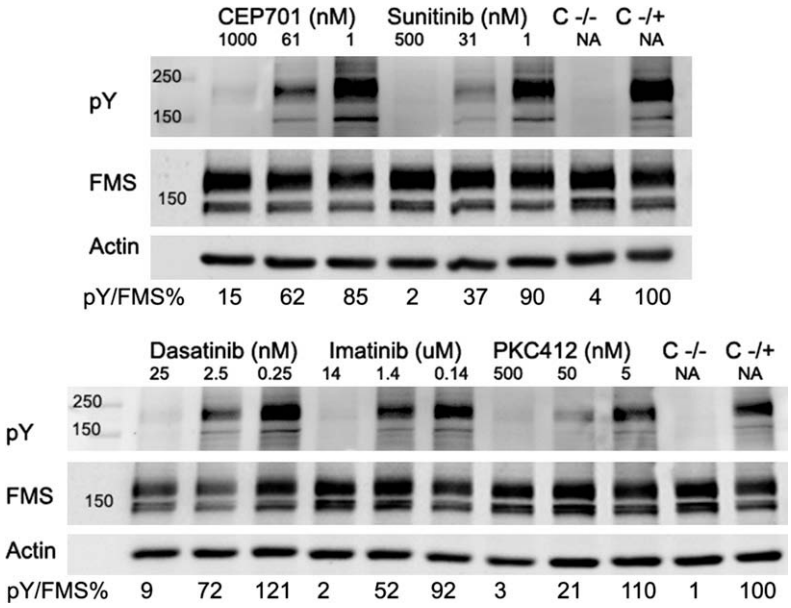


**Figure 4.** Inhibition of CSF-1-dependent FMS autophosphorylation by small molecule inhibitors. FD-FMS cells starved of growth factor for 3 h were pre-treated with the indicated concentrations of drugs then pulsed with CSF-1. Cells were lysed, proteins separated by PAGE and western blots developed with antibodies to phosphotyrosine (pY), FMS and actin (loading control). C−/+ indicates cells stimulated with CSF-1 in the absence of drug. C−/− indicates the unstimulated, no drug, control. Numbers below each track indicate the ratio of pY/FMS band intensity normalised to the positive control.

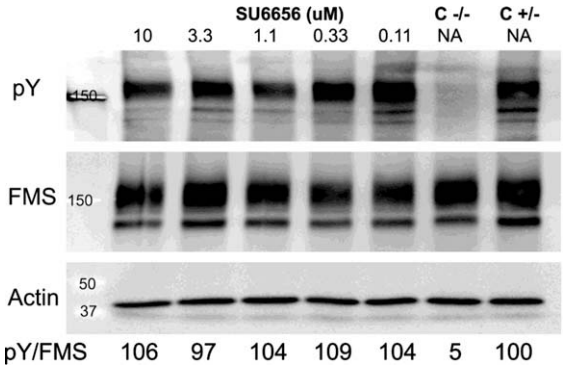


**Figure 5.** Effect of the SFK inhibitor, SU6656, on CSF-1-dependent FMS autophosphorylation. The experiment was conducted as described for Figure 4.

structures of the FMS kinase domain. These were prepared by removing the existing ligand from the crystal structure of FMS or by homology modelling based on crystal structures of an inhibitor or ADP (as an ATP mimic) bound to a related tyrosine kinase. This approach allowed docking of each inhibitor into both active and inactive FMS kinase conformations. The approach also allowed docking into a 'pre-formed' binding pocket suitable for that inhibitor. For example, the crystal structure of FMS in complex with arylamide (2I1M), which is similar in size and shape to CEP-701 and to PKC-412 (Fig. 1), was used for the docking of these inhibitors. On the other hand, imatinib could not be docked into this structure and was therefore docked into a homology model based on the crystal structure of the KIT/imatinib complex. Furthermore, the use of this approach provided an explanation (steric clash with M637) for the higher $IC_{50}$ for imatinib for FMS compared with KIT inhibition.[11,18] Similarly, dacatinib (a modified form of dasatinib; Fig. 1) and sunitinib were successfully docked into homology models of the FMS kinase based on the crystal structures of the Abl/dasatinib and KIT/sunitinib complexes.

Docking results were compared with measurement of $IC_{50}$ in cell-based assays of FMS function. The cell line model used to measure inhibition of cell growth enables us to determine selectivity of the inhibitor for FMS signalling in response to CSF-1 by comparison with FMS-independent growth in GM-CSF. Imatinib, dasatinib and sunitinib showed selectivity for FMS signalling whereas CEP-701 and PKC-412 inhibited growth in GM-CSF to a similar extent. The GM-CSF receptor is a member of the cytokine receptor family, lacks intrinsic kinase activity and is dependent on an associated JAK kinase for signalling.[29] The results indicate that CEP-701 and PKC-412 also inhibit JAK and/or downstream kinases leading to cell survival and proliferation in response to GM-CSF. Some of these kinases may also be involved in signalling downstream of FMS. However, analysis of FMS autophosphorylation in response to CSF-1 provided confirmation that all five compounds directly inhibited FMS kinase, supporting the docking results. We found no strong correlation between the energy of docking and the $IC_{50}$ values in cell-based functional assays. This is not surprising for two main reasons: Firstly, as discussed already, we have not taken the induced fit upon inhibitor binding into account when docking. Secondly, docking only considers the binding between the kinase and the small molecule inhibitor, whereas the cell-based assays also depend on other factors, such as cellular uptake of the inhibitors.

The binding site for kinase inhibitors is located in the cleft between the N- and C-terminal lobes. This cleft has two main regions: the hinge region occupied by ATP in the active conformation at the very end of the cleft, as observed in the KIT/ADP complex crystal structure, and the catalytic region between C-$\alpha$ helix and activation loop at the entrance of the cleft. The catalytic region undergoes dramatic conformational changes during kinase activation, but apart from repositioning of the Phe side chain in the DFG motif at the beginning of the activation loop, the conformation of the hinge region is similar in both active and inactive conformations of the kinase domain. As a result, the activity of small molecule inhibitors against active, inactive or both conformations of kinase domains will largely depend on whether they bind to the hinge region or catalytic area.

Based on our docking results, imatinib, dasatinib and CEP-701 represent three different types of interactions, which determine their potency and selectivity, as confirmed in our experimental assays. Interaction with the hinge region and occupation of the ATP space, particularly the space taken up by the adenine ring system, is the common feature for all compounds studied here, and all apart from sunitinib, form a hydrogen bond with Cys666 in the hinge region. Interaction with the corresponding residues in other kinases (e.g., Met318 in Abl and Cys673 in KIT) is a common feature of ATP-competitive inhibitors.

Imatinib, a relatively potent and selective molecule, extends well into the entrance of the binding cleft and its activity is restricted to the inactive conformation of kinases.[32] Similarly, sunitinib proved to be a moderately potent and fairly selective inhibitor in our model system. The crystal structure on which our homology model was based shows part of sunitinib bound to the inactive conformation of KIT.[24] Sunitinib could not be docked very well into our FMS model of the inactive conformation. Like imatinib, sunitinib could not be docked into the ATP-binding pocket of the FMS active conformation model, and fails to inhibit constitutively active KIT kinase domain mutants.[24] The $IC_{50}$ values indicate that sunitinib is about eight times more potent in inhibiting growth in CSF-1 than in GM-CSF. It is not highly selective in other systems and inhibits other kinases and transporters.[33]

Dasatinib was a highly potent and selective inhibitor of FMS in our system, although it also inhibits SFKs, KIT and Abl kinase.[17,34] Dacatinib, used here for docking, and demonstrated to be a good model for dasatinib, interacts mainly with the hinge region, and extends into the catalytic region, but not into the region of highest conformational change. Structural studies have indicated that dasatinib can bind to both active and inactive conformations of Abl kinase, probably accounting for its potency.[23] Accordingly, dasatinib inhibits inactive and some active forms of kinases including imatinib-resistant Abl kinase However, Thr315 mutants (equivalent to Thr663 in FMS) are resistant to dasatinib because this residue is involved in dasatinib binding.[23] A hydrogen bond interaction between dacatinib and the relevant Thr was observed in our docking study for the model of the active FMS conformation and for the Abl kinase in the active conformation.

CEP-701 is a potent, non-selective inhibitor, interacts exclusively with the ATP-binding pocket in the hinge region, and occupies all the space taken by ATP. Low selectivity of CEP-701 and PKC-412 may occur because this area is highly conserved among different kinases. The likelihood of developing resistance against these types of inhibitors is reduced, because mutations in the ATP-binding pocket may result in loss of kinase function. PKC-412 and CEP-701 are effective against some mutants[30,35] and can be considered as lead compounds for developing inhibitors against constitutively active mutant kinases. CEP-701, the smaller, more potent FMS inhibitor, can according to our docking results, bind to both the active and inactive FMS conformations.

## 4. Conclusion

Docking of imatinib, dasatinib and CEP-701 into the FMS kinase domain demonstrated different types of interactions that correlated with inhibitor potency and selectivity in cell-based assays of FMS function. The structure–activity relationships determined

here will be useful in designing more potent and selective drugs for treatment of diseases not only associated with FMS, but also other kinases. The core structure of a heteroaromatic ring system (to mimic adenine) interacting with the hinge region (Cys666 of FMS or corresponding residue in the other kinases) is the starting point for designing any new small molecule kinase inhibitor. Extension of the molecule towards the catalytic area, including the gatekeeper residue (Thr663 in FMS), can then increase selectivity, but renders the molecule more vulnerable to the conformational changes upon activation of the kinase. On the other hand, extension of the core structure towards residues interacting with the phosphate groups of ATP results in decreasing selectivity but creates molecules that can interact with both the active and inactive conformations of the kinase domain. Where minimisation of side effects due to inhibition of a broad range of kinases is of crucial importance, high selectivity can be achieved by targeting parts of the ATP-binding pocket interacting with adenine and parts of the catalytic area, which are less conserved among kinases. Conversely, targeting the ATP-binding pocket in the hinge region may have some advantages in overcoming the resistance associated with activating mutations in the kinase domain but is likely to result in less selectivity.

## 5. Experimental

### 5.1. Homology modelling

Homology models of FMS were built as described previously[36] based on crystal structures of 1T46, KIT with imatinib,[21] 2GQG, Abl kinase with dasatinib,[23] 3G0E, KIT with sunitinib,[24] and 1PKG, an active conformation of KIT with ADP,[25] obtained from the RCSB Protein Data Bank (PDB) as templates. SWISS-MODEL and the Swiss-PdbViewer were used for preparation and evaluation of the models.[37] The models were used for docking of imatinib, dasatinib and sunitinib without any further minimisation or modification.

### 5.2. Docking procedure

AutoDock Tools (ADT)[38] was used for preparation of Ligand.out.pdbqt and protein.pdbqs files containing ligand torsions and solvent parameters for the protein, respectively, as well as grid and docking parameter files. Some of the docking default values of ADT were changed to optimise the docking results. Population size was increased up to 5000; the number of energy evaluations up to $1 \times 10^7$, and the number of runs up to 100. Crystal structures of FMS[22] and KIT (21IM and 1T46) were superimposed on each other to define a grid box to accommodate both the arylamide molecule and imatinib. This grid box was used for evaluation of the docking procedure in which the ligand was taken out and docked back into its protein crystal structure. The grid box size was $60 \times 60 \times 68$ points, where grid spacing was 0.375 Å. The centre of the grid was determined as the centre of all residues within 5 Å distance from the ligands in superimposed structures using Discovery Studio Visualizer (DSV) software (Accelrys, CA, USA). Superimpositions were performed in DSV using sequence alignments obtained during homology modelling. All aligned Cα atoms were superimposed. AutoGrid 3 and AutoDock 3.05 programs[39–41] were used for calculation of grid maps and final docking. Docking results were analysed for the number of clusters, average binding energy of each cluster, and the interactions between docked poses of ligand and protein macromolecule using ADT. A pdb file was extracted from each docking log file containing the coordinates of the lowest energy pose in each cluster for further analysis by DSV.

### 5.3. CSF-1 production

The coding region for residues 33–182 of human CSF-1 was amplified using cDNA made from K562 cells and cloned into the pPICZαA expression vector (Invitrogen, Carlsbad, CA). The construct was electroporated into *Pichia Pastoris* (Invitrogen) and CSF-1 expression induced in BMMY media with 2% methanol. Biological activity of product (human recombinant CSF-1) in the yeast supernatant was validated by comparison with commercial human recombinant CSF-1 (PeproTech, Rocky Hill, NJ) in supporting proliferation of FDC-P1 cells expressing human FMS (FD-FMS cells) and promoting FMS tyrosine phosphorylation in THP-1 cells.

### 5.4. FMS expression

The factor-dependent murine early myeloid cell line FDC-P1 (ATCC No. CRL-12103) was routinely maintained in DMEM/10% FCS supplemented with murine GM-CSF as previously described.[26] Where indicated FDC-P1 cells that had been transduced with FMS cDNA (FD-FMS cells) were grown in CSF-1 instead of GM-CSF. The MSCV-FMS-IRES-GFP construct was supplied by Dr. A.B. Lyons, Hanson Institute, Adelaide, with the consent of the originator Dr M. Roussel, St. Jude Children's Research Hospital, Memphis; TN. DNA was introduced into FDC-P1 cells by retrovirus-mediated gene transfer as previously described.[30] FDC-P1 cells expressing FMS (FD-FMS) were selected using CSF-1 as growth factor and sorted (FACS Aria, BD Biosciences, CA) for expression of GFP to get a homogenous population. FMS expression on sorted cells was confirmed by flow cytometry using c-FMS/CSF-1R (C-20) antibody (Santa Cruz Biotechnology, Santa Cruz, CA) and sheep anti-mouse IgG conjugated with PE (Chemicon, Billerica, MA) as secondary antibody.

### 5.5. Cell proliferation assay

Serial dilutions of kinase inhibitors imatinib and PKC-412 (Novartis, Basel, Switzerland), dasatinib and sunitinib (Chemietek, Indianapolis, IN) and CEP-701 (LC Laboratories, Woburn, MA) were prepared from 10 mM stock solutions of each drug in dimethyl sulfoxide (DMSO, Ajax Finechem, NSW, Australia) in 100 μl DMEM containing 10% FCS and either 2× CSF-1 or GM-CSF in 96 well plates (Nunc, Roskilde, Denmark). FD-FMS cells ($5 \times 10^4$) in 100 μl growth factor free medium were added to each well. Plates were incubated at 37 °C with 5% $CO_2$ for 48 h. Resazurin reagent containing 300 μM resazurin, 78 μM methylene blue, 1 mM potassium hexacyanoferrate III and 1 mM potassium hexacyanoferrate II (all from Sigma, St. Louis, MO) was added (20 μl into each well) and the plates were incubated for 4 h. Fluorescence intensity of the product resorufin, proportional to the number of viable cells per well, was measured by a FLUOstar OPTIMA (BMG LABTECH, Offenburg, Germany) with excitation at 530 nm and emission at 590 nm. Results were analysed using GraphPad Prism 4.3 for Windows, (GraphPad Software, San Diego, CA) and the $IC_{50}$ was determined by fitting a non-linear curve into all data points of fluorescence graphed against logarithm of drug concentration.

### 5.6. Inhibition of autophosphorylation

FD-FMS cells were grown in the presence of murine GM-CSF to density of $10^6$ cells/ml, washed, resuspended in FCS- and GF-Free medium and incubated for 3 h at 37 °C. Then $10^7$ cells were added to 1 ml of FCS- and GF-free medium containing different concentrations of drugs and incubated for 30 min at 37 °C. Cells were cooled on ice then stimulated with CSF-1 for 5 min. This protocol gives optimum phosphorylation and minimal degradation of FMS.[42] The cells were lysed with ice-cold 1% NP40 in TSE (50 mM

Tris–HCl, 150 mM NaCl, 1 mM EDTA pH8.0) with complete protease inhibitor cocktail (Roche, Basel, Switzerland), 5 mM sodium fluoride, 5 mM tetra sodium pyrophosphate, 5 mM sodium vanadate, and 1 mM phenylmethylsulfonyl fluoride (Sigma). Lysates were centrifuged to remove cell debris and protein concentration determined using a MicroBCA kit (Pierce, Rockford, IL). Samples (50 μg of protein) were run on 6% SDS/polyacrylamide gels under reduced conditions along with Precision Plus protein Standards (BioRad, Hercules, CA). Separated samples were transferred to nitrocellulose membrane. The membrane was blocked with 1% BSA (Sigma) for 1 h and probed for phosphotyrosine using a cocktail of 4G10 (Upstate, Temecula, CA) and pY20 (BD Biosciences) antibodies, FMS (sc-692 antibody; Santa Cruz Biotechnology) or actin (Sigma). Bound antibody was detected with secondary anti-mouse or anti-rabbit IgG antibody conjugated with HRP and ECL. Chemiluminence was measured using a Fuji imaging system (Fujifilm, Tokyo, Japan) and quantitated using Multi Gauge V3 software (Fujifilm).

## Acknowledgements

The authors would like to thank Mr David Huthnance and Mr Michael Brown for their assistance with setting up AutoDock at the School of Environmental and Life Sciences, University of Newcastle. This work has been supported by a grant to L.K.A. from The Anthony Rothe Memorial Trust. Infrastructure funding was provided by the New South Wales Office of Science and Medical Research through the Hunter Medical Research Institute. L.K.A. is a Principal Research Fellow supported by the National Health and Medical Research Council of Australia.

## References and notes

1. Hubbard, S. R.; Till, J. H. *Annu. Rev. Biochem.* **2000**, *69*, 373.
2. Roth, P.; Stanley, E. R. *Curr. Top. Microbiol. Immunol.* **1992**, *181*, 141.
3. Ide, H.; Seligson, D. B.; Memarzadeh, S.; Xin, L.; Horvath, S.; Dubey, P.; Flick, M. B.; Kacinski, B. M.; Palotie, A.; Witte, O. N. *Proc. Natl. Acad. Sci. U.S.A.* **2002**, *99*, 14404.
4. Sapi, E. *Exp. Biol. Med.* **2004**, *229*, 1.
5. Irvine, K. M.; Andrews, M. R.; Fernandez-Rojo, M. A.; Schroder, K.; Burns, C. J.; Su, S.; Wilks, A. F.; Parton, R. G.; Hume, D. A.; Sweet, M. J. *J. Leukocyte Biol.* **2009**, *85*, 278.
6. Takayanagi, H.; Oda, H.; Yamamoto, S.; Kawaguchi, H.; Tanaka, S.; Nishikawa, T.; Koshihara, Y. *Biochem. Biophys. Res. Commun.* **1997**, *240*, 279.
7. Chitu, V.; Stanley, E. R. *Curr. Opin. Immunol.* **2006**, *18*, 39.
8. Yee, L. D.; Liu, L. *Anticancer Res.* **2000**, *20*, 4379.
9. Kluger, H. M.; Dolled-Filhart, M.; Rodov, S.; Kacinski, B. M.; Camp, R. L.; Rimm, D. L. *Clin. Cancer Res.* **2004**, *10*, 173.
10. Savarese, D. M.; Valinski, H.; Quesenberry, P.; Savarese, T. *Prostate* **1998**, *34*, 80.
11. Brownlow, N.; Russell, A. E.; Saravanapavan, H.; Wiesmann, M.; Murray, J. M.; Manley, P. W.; Dibb, N. J. *Leukemia* **2008**, *22*, 649.
12. Brownlow, N.; Mol, C.; Hayford, C.; Ghaem-Maghami, S.; Dibb, N. J. *Leukemia* **2009**, *23*, 590.
13. Dewar, A. L.; Farrugia, A. N.; Condina, M. R.; Bik To, L.; Hughes, T. P.; Vernon-Roberts, B.; Zannettino, A. C. *Blood* **2006**, *107*, 4334.
14. Vandyke, K.; Dewar, A. L.; Farrugia, A. N.; Fitter, S.; Bik To, L.; Hughes, T. P.; Zannettino, A. C. *Leukemia* **2009**, *23*, 994.
15. Hiraga, T.; Nakamura, H. *Int. J. Cancer* **2008**, *124*, 215.
16. Nam, S.; Kim, D.; Cheng, J. Q.; Zhang, S.; Lee, J. H.; Buettner, R.; Mirosevich, J.; Lee, F. Y.; Jove, R. *Cancer Res.* **2005**, *65*, 9185.
17. Druker, B. J. *Oncogene* **2002**, *21*, 8541.
18. Dewar, A. L.; Cambareri, A. C.; Zannettino, A. C.; Miller, B. L.; Doherty, K. V.; Hughes, T. P.; Lyons, A. B. *Blood* **2005**, *105*, 3127.
19. Buchdunger, E.; Cioffi, C. L.; Law, N.; Stover, D.; Ohno-Jones, S.; Druker, B. J.; Lydon, N. B. *J. Pharmacol. Exp. Ther.* **2000**, *295*, 139.
20. Guo, T.; Agaram, N. P.; Wong, G. C.; Hom, G.; D'Adamo, D.; Maki, R. G.; Schwartz, G. K.; Veach, D.; Clarkson, B. D.; Singer, S.; DeMatteo, R. P.; Besmer, P.; Antonescu, C. R. *Clin. Cancer Res.* **2007**, *13*, 4874.
21. Mol, C. D.; Dougan, D. R.; Schneider, T. R.; Skene, R. J.; Kraus, M. L.; Scheibe, D. N.; Snell, G. P.; Zou, H.; Sang, B. C.; Wilson, K. P. *J. Biol. Chem.* **2004**, *279*, 31655.
22. Schubert, C.; Schalk-Hihi, C.; Struble, G. T.; Ma, H. C.; Petrounia, I. P.; Brandt, B.; Deckman, I. C.; Patch, R. J.; Player, M. R.; Spurlino, J. C.; Springer, B. A. *J. Biol. Chem.* **2007**, *282*, 4094.
23. Tokarski, J. S.; Newitt, J. A.; Chang, C. Y.; Cheng, J. D.; Wittekind, M.; Kiefer, S. E.; Kish, K.; Lee, F. Y.; Borzillerri, R.; Lombardo, L. J.; Xie, D.; Zhang, Y.; Klei, H. E. *Cancer Res.* **2006**, *66*, 5790.
24. Gajiwala, K. S.; Wu, J. C.; Christensen, J.; Deshmukh, G. D.; Diehl, W.; DiNitto, J. P.; English, J. M.; Greig, M. J.; He, Y. A.; Jacques, S. L.; Lunney, E. A.; McTigue, M.; Molina, D.; Quenzer, T.; Wells, P. A.; Yu, X.; Zhang, Y.; Zou, A.; Emmett, M. R.; Marshall, A. G.; Zhang, H. M.; Demetri, G. D. *Proc. Natl. Acad. Sci. U.S.A.* **2009**, *106*, 1542.
25. Mol, C. D.; Lim, K. B.; Sridhar, V.; Zou, H.; Chien, E. Y.; Sang, B. C.; Nowakowski, J.; Kassel, D. B.; Cronin, C. N.; McRee, D. E. *J. Biol. Chem.* **2003**, *278*, 31461.
26. Frost, M. J.; Ferrao, P. T.; Hughes, T. P.; Ashman, L. K. *Mol. Cancer Ther.* **2002**, *1*, 1115.
27. Das, J.; Chen, P.; Norris, D.; Padmanabha, R.; Lin, J.; Moquin, R. V.; Shen, Z.; Cook, L. S.; Doweyko, A. M.; Pitt, S.; Pang, S.; Shen, D. R.; Fang, Q.; de Fex, H. F.; McIntyre, K. W.; Shuster, D. J.; Gillooly, K. M.; Behnia, K.; Schieven, G. L.; Wityak, J.; Barrish, J. C. *J. Med. Chem.* **2006**, *49*, 6819.
28. Blake, R. A.; Broome, M. A.; Liu, X.; Wu, J.; Gishizky, M.; Sun, L.; Courtneidge, S. A. *Mol. Cell Biol.* **2000**, *20*, 9018.
29. Watanabe, S.; Itoh, T.; Arai, K. *Leukemia* **1997**, *11*, 76.
30. Roberts, K. G.; Odell, A. F.; Byrnes, E. M.; Baleato, R. M.; Griffith, R.; Lyons, A. B.; Ashman, L. K. *Mol. Cancer Ther.* **2007**, *6*, 1159.
31. Griffith, R.; Brown, M. N.; McCluskey, A.; Ashman, L. K. *Mini-Rev. Med. Chem.* **2006**, *6*, 1101.
32. Schindler, T.; Bornmann, W.; Pellicena, P.; Miller, W. T.; Clarkson, B.; Kuriyan, J. *Science* **2000**, *289*, 1938.
33. Shukla, S.; Robey, R. W.; Bates, S. E.; Ambudkar, S. V. *Drug Metab. Dispos.* **2009**, *37*, 359.
34. Schittenhelm, M. M.; Shiraga, S.; Schroeder, A.; Corbin, A. S.; Griffith, D.; Lee, F. Y.; Bokemeyer, C.; Deininger, M. W.; Druker, B. J.; Heinrich, M. C. *Cancer Res.* **2006**, *66*, 473.
35. Knapper, S.; Mills, K. I.; Gilkes, A. F.; Austin, S. J.; Walsh, V.; Burnett, A. K. *Blood* **2006**, *108*, 3494.
36. Foster, R.; Griffith, R.; Ferrao, P.; Ashman, L. *J. Mol. Graphics Modell.* **2004**, *23*, 139.
37. Guex, N.; Peitsch, M. C. *Electrophoresis* **1997**, *18*, 2714.
38. Sanner, M. F. *J. Mol. Graphics Modell.* **1999**, *17*, 57.
39. Morris, G. M.; Goodsell, D. S.; Halliday, R. S.; Huey, R.; Hart, W. E.; Belew, R. K.; Olson, A. J. *J. Comput. Chem.* **1998**, *19*, 1639.
40. Morris, G. M.; Goodsell, D. S.; Huey, R.; Olson, A. J. *J. Comput. Aided Mol. Des.* **1996**, *10*, 293.
41. Goodsell, D. S.; Olson, A. J. *Proteins* **1990**, *8*, 195.
42. Yeung, Y. G.; Stanley, E. R. *Mol. Cell. Proteomics* **2003**, *2*, 1143.